

Bayesian inference of thermal effects in dense matter

Adriana R. Raduta

(araduta@nipne.ro)

Collaborator: Mikhail Beznogov (IFIN-HH, Bucharest)

Beznogov & Raduta, Phys. Rev. C 107, 045803 (2023)

Raduta, Beznogov & Oertel, arXiv: 2402.14593



ECT*, Trento, 22-26 April, 2024



- EOS in the era of multimessenger astrophysics
- C(ovariant) D(ensity) F(unctional) EOS for cold and dense matter: a Bayesian approach
 - model dependence of the results
 - correlations with parameters of N(uclear) M(atter)
- Thermal effects on thermal energy density and pressure, entropy per baryon, heat capacities at constant volume and pressure, adiabatic and thermal index, speed of sound in CDF EOS
 - correlations with effective Dirac mass
 - pseudo-Sommerfeld expansion
 - test of alternative Sommerfeld expansion [Constantinou+, Ann. Phys. (2015)]
- Conclusions

Phenomenological EOS in the era of multimessenger astrophysics (I)

- EOS - an essential ingredient for atomic nuclei, NM and NS
- EOS - built from effective interactions designed to comply with the symmetry properties of the space; with parameters tuned such as to describe nuclear data (masses, charge r.m.s. radii, neutron skin thicknesses, charge radii diff. in mirror nuclei, energy of giant monopole/dipole/quadrupole resonances, dipole polarizability, flow and particle production in heavy ion collisions, etc.)
e.g.: Skyrme, Gogny, MDI, CDF
- well known around $(n_{\text{sat}}, \delta = 0)$ with $n_{\text{sat}} \sim 2.7 \cdot 10^{14} \text{g/cm}^3 \sim 0.16 \text{fm}^{-3}$ and $\delta = (n_n - n_p)/n$
- uncertain at high densities and isospin asymmetries

Phenomenological EOS in the era of multimessenger astrophysics (II)

- availability of NS data, e.g., $M_G/M_\odot \gtrsim 2$ [1], tidal deformabilities [2], radii [3], resulted in a renaissance; better constraints at (n, δ) not accessible so far
- situation is still difficult: few data; large error bars; dependence on NS mass and the unknown EOS, different density domains are explored; every global param. depends in a specific and convoluted way on the EOS behavior over different density domains
- complexity & uncertainties best handled in statistical approaches, e.g., Bayesian

[1] Antoniadis+, Science (2013); Arzoumanian+, ApJSS (2018); Cromartie+, Nature (2020); Fonseca+, ApJL (2021) [2] Abbott+, PRL (2017); Abbott+, PRX (2019) [3] Miller+, ApJL (2019); Riley+, ApJL (2019); Miller+, ApJL (2021); Riley+, ApJL (2021); Vinciguerra+, ApJ (2024)

Bayesian inferences of EOSs for cold and dense matter

- Phenomenological models successfully used in nuclear physics are employed:
 - non-relativistic models with Skyrme effective interactions [1],
 - CDF with D(ensity) D(ependent) and non-linear couplings [2]
- Constraints: nuclear empirical parameters (NEP), χ EFT calculations of P(pure) N(eutron) (M)atter, astro. measurements of NSs; various combinations
- Conclusions: EOS, properties of NSs, global parameters of NSs, correlations depend on priors, sets of constraints, structure of the density functional

... In the following, CDF with DD couplings will be considered

[1] Zhou, Xu & Papakonstantinou, PRC (2023); Beznogov & Raduta, ApJ (2024); Beznogov & Raduta, arXiv:2403.19325

[2] Malik+, ApJ (2022); Malik+, PRD (2023); Beznogov & Raduta, PRC (2023); Char+, PRD (2023)

Covariant Density Functional model with Density Dependent couplings

Lagrangian density [1,2]: $\mathcal{L}(\sigma, \omega, \rho; \Gamma_\sigma, \Gamma_\omega, \Gamma_\rho)$

Density-dependent couplings [3]: $\Gamma_M(n) = \Gamma_{M,0} h_M(x)$, $x = n/n_{\text{sat}}$, with

$$h_M(x) = \exp[-(x^{a_M} - 1)], \quad M = \sigma, \omega; \quad h_\rho(x) = \exp[-a_\rho(x - 1)]$$

6 parameters: $\Gamma_{\sigma,0}$, $\Gamma_{\omega,0}$, $\Gamma_{\rho,0}$, a_σ , a_ω , a_ρ

[1] Walecka, Ann. Phys. (1974); [2] Typel & Wolter, Nucl. Phys. A (1999); [3] Malik, Ferreira, Agrawal & Providencia, Ap.J. (2022)

Constraints

Quantity	Units	Value	Std. deviation	Ref.
n_{sat}	fm^{-3}	0.153	0.005	[1]
E_{sat}	MeV	-16.1	0.2	[2]
K_{sat}	MeV	230	40	[3,4]
J_{sym}	MeV	32.5	1.8	[5]
P_1	MeV/fm^3	0.509	2×0.093	[6]
P_2	MeV/fm^3	1.238	2×0.302	[6]
P_3	MeV/fm^3	2.482	2×0.687	[6]
M_{G}^*	M_{\odot}	> 2.0	—	[7]

NM parameters;

density behavior of PNM as predicted by χEFT ; 1, 2, 3: $n_B = 0.08, 0.12, 0.16 \text{ fm}^{-3}$

astro. constraint

[1] Typel & Wolter, NuclPhysA (1999); [2] Dutra+, PhysRevC (2014); [3] Todd-Rutel & Piekarewicz, PhysRevLett (2005); [4] Shlomo+, EPJA (2006); [5] Essik+, PhysRevC (2021); [6] Hebeler+, ApJ (2013); [7] Fonseca+, ApJL (2021);

Priors, Likelihood

Priors: uniform (uninformative) distributions [1]

Likelihood: $\log \mathcal{L}_q \propto -\chi_q^2 = -\sum_{n=1}^N \chi_n^2 - \chi_{\text{thr}}'^2$.

1) Uncorrelated obs., e.g., n_{sat} , E_{sat} , K_{sat} , L_{sym} , $(E/A)_i$:

$$-\chi_n^2 = -\frac{1}{2} \left(\frac{d_i - \xi_i(\Theta)}{\mathcal{X}_i} \right)^2$$

2) "Hard-wall" (threshold), M_G^* : $-\chi_{\text{thr}}'^2 = -10^{10}$, if $M_G^*/M_\odot < 2$

[1] Malik, Ferreira, Agrawal & Providencia, ApJ (2022)

Marginalized posterior distributions (I): NM parameters

Quantity	Units	Med.	68% CI	Data	Ref.
n_{sat}	fm^{-3}	0.153	+0.0049 -0.0049	0.153 ± 0.005	[1]
E_{sat}	MeV	-16.1	+0.2 -0.2	-16.1 ± 0.2	[2]
K_{sat}	MeV	247	+33 -28	230 ± 40	[3,4]
Q_{sat}	MeV	-39.9	+160 -130	-	
Z_{sat}	MeV	1360	+410 -830	-	
J_{sym}	MeV	32.1	+1.8 -1.8	32.5 ± 1.8	[5]
L_{sym}	MeV	42.3	+15 -13	-	
K_{sym}	MeV	-105	+27 -24	-	
Q_{sym}	MeV	932	+360 -420	-	
Z_{sym}	MeV	-6440	+3100 -3800	-	
m_{eff}	m_{N}	0.657	+0.041 -0.045	0.55 ± 0.05	[6]
P_1	MeV/fm^3	0.537	+0.1 -0.12	0.509 ± 0.186	[7]
P_2	MeV/fm^3	1.2	+0.39 -0.39	1.238 ± 0.604	[7]
P_3	MeV/fm^3	2.67	+0.82 -0.72	2.482 ± 1.374	[7]

[1] Typel & Wolter, NuclPhysA (1999); [2] Dutra+, PhysRevC (2014); [3] Todd-Rutel & Piekarezcic, PhysRevLett (2005); [4] Shlomo+, EPJA (2006); [5] Essik+, PhysRevC (2021); [6] Typel, PhysRevC (2005); [7] Hebel+., ApJ (2013);

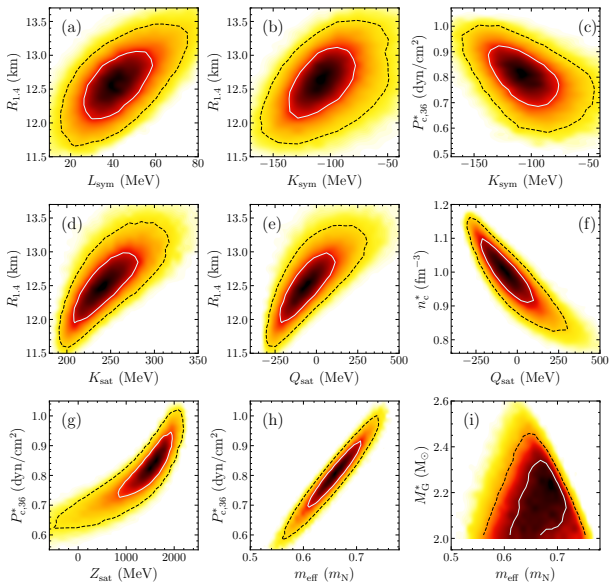
Marginalized posterior distributions (II): NS parameters

Quantity	Units	Med.	68% CI	Obs.	Ref.
M_G^*	M_\odot	2.16	+0.15 -0.11	$\gtrsim 2$	[1]
M_B^*	M_\odot	2.57	+0.2 -0.15	-	-
n_c^*	fm^{-3}	0.98	+0.079 -0.083	-	-
$\rho_{c,15}^*$	10^{15}g/cm^3	2.21	+0.19 -0.18	-	-
$P_{c,36}^*$	10^{36}dyn/cm^2	0.798	+0.091 -0.097	-	-
$R_{1.4}$	km	12.6	+0.42 -0.42	12.45 ± 0.65	[2]
$\Lambda_{1.4}$	-	519	+120 -100	190_{-120}^{+390} *	[3]
$R_{2.0}$	km	12.2	+0.62 -0.64	12.35 ± 0.75	[2]
M_{DU}	M_\odot	-	-	-	-

[1] Fonseca+, ApJL (2021); [2] Miller+, ApJLett (2021); [3] Abbott+, PhysRevLett (2018)

* at 90% CI

Correlations between NM and NS params



- $R_{1.4} - L_{\text{sym}}$ (very weak)
- $R_{1.4} - K_{\text{sat}}, Q_{\text{sat}}$ (weak)
- $P_c^* - Z_{\text{sat}}; n_c^* - Q_{\text{sat}}$ (weak)
- $P_c^* - m_{\text{eff}}$ (strong)

Finite temperature EOSs

- simulations of core-collapse supernovae, proto-NS evolution, BNS mergers, stellar BH formation require 3D EOSs; values of state variables and microscopic quantities are provided for wide domains of baryonic density [$10^{-10} \leq n_B \leq 1 - 10 \text{ fm}^{-3}$], temperature [$0 \leq T \leq 100 \text{ MeV}$] and charge fraction [$0 \leq Y_Q \leq 0.6$]
- many such EOSs are available*; based on ab initio/relativistic/non-relativistic approaches; account for different properties of NM (K_{sat} , E_{sym} , L_{sym} , etc.); various compositions (nucleonic, admixtures of hyperons, Δ s, π , K , quarks)

Question: which properties of NM govern the finite- T behavior?

- In this talk:**
- CDFs with DD couplings;
 - correlations between e_{th} , p_{th} , S/A , Γ_{th} , Γ_S , C_V , C_P , c_S^2 and Dirac mass;
 - the 10^5 models of run 1 in Ref. [1] are considered;
 - $n = 0.15, 0.6 \text{ fm}^{-3}$, $T = 20, 50 \text{ MeV}$ and $Y_Q = 0.5$

* <https://compose.obspm.fr/>

[1] Beznogov & Raduta, Phys.Rev.C (2023)

Energy density and pressure:

$$e = e_{\text{kin}} + e_{\text{int}},$$

$$p = p_{\text{kin}} + p_{\text{int}} + p_{\text{rearrang}}.$$

Kinetic terms:

$$e_{\text{kin}} = \sum_{i=n,p} \frac{1}{\pi^2} \int_0^\infty dk k^2 E_i(k) f_{\text{FD}}(E_i(k) - \mu_i^*),$$

$$p_{\text{kin}} = \frac{1}{3} \sum_{i=n,p} \frac{1}{\pi^2} \int_0^\infty \frac{dk k^4}{E_i(k)} f_{\text{FD}}(E_i(k) - \mu_i^*).$$

Interaction terms:

$$e_{\text{int}} = \frac{m_\sigma^2}{2} \bar{\sigma}^2 + \frac{m_\omega^2}{2} \bar{\omega}^2 + \frac{m_\rho^2}{2} \bar{\rho}^2,$$

$$p_{\text{int}} = -\frac{m_\sigma^2}{2} \bar{\sigma}^2 + \frac{m_\omega^2}{2} \bar{\omega}^2 + \frac{m_\rho^2}{2} \bar{\rho}^2.$$

Mean field expectations:

$$m_\sigma^2 \bar{\sigma} = \sum_{i=n,p} \Gamma_\sigma n_i^s,$$

$$m_\omega^2 \bar{\omega} = \sum_{i=n,p} \Gamma_\omega n_i,$$

$$m_\rho^2 \bar{\rho} = \sum_{i=n,p} \Gamma_\rho t_{3i} n_i,$$

where

$$n_i^s = \frac{1}{\pi^2} \int_0^\infty \frac{dk k^2 m_i^*}{E_i(k)} f_{\text{FD}}(E_i(k) - \mu_i^*),$$

$$n_i = \frac{1}{\pi^2} \int_0^\infty dk k^2 f_{\text{FD}}(E_i(k) - \mu_i^*).$$

$$\text{with } E_i(k) = \sqrt{k^2 + m_i^{*2}}.$$

CDF at finite temperature

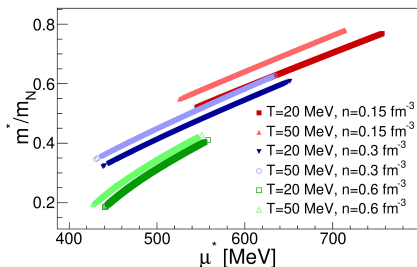
effective chemical potential

$$\mu_i^* = \mu_i - \Gamma_\omega \bar{\omega} - \Gamma_\rho t_{3i} \bar{\rho} - \Sigma_R,$$

and effective mass $m_i^* = m_N - \Gamma_\sigma \bar{\sigma}$

are linked via

$$n_i = \frac{1}{\pi^2} \int_0^\infty dk k^2 f_{\text{FD}}(E_i(k) - \mu_i^*).$$



$\Rightarrow e_{\text{th}}, p_{\text{th}}$, etc. depend on m^*

μ^* and m^* are n and T -dependent

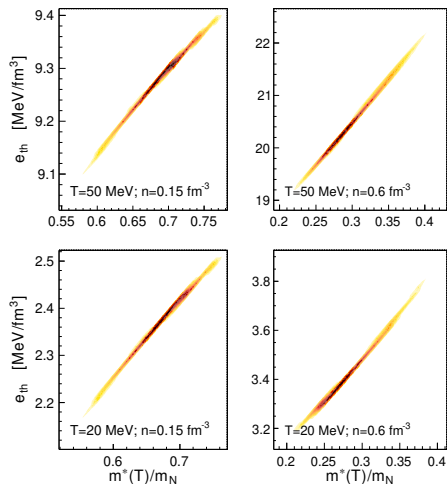
T -modifications are comparable

In non-rel. models, thermal eff. are determined by the Landau mass [1]

[1] Constantinou+, PhysRevC (2014); ibid. (2015)

Thermal energy

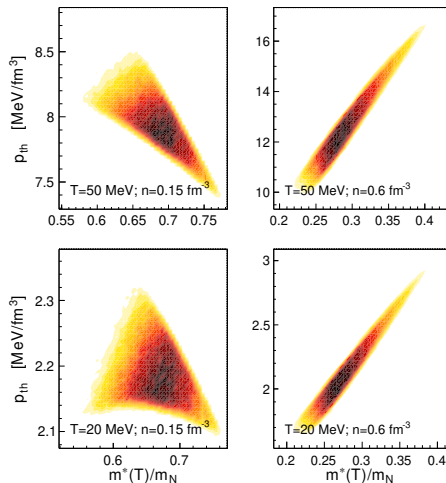
$$e_{\text{th}} = e(n, Y_p, T) - e(n, Y_p, T = 0)$$



- excellent, almost linear scaling with the Dirac effective mass;
- can be understood within the low- T approximation, but persists beyond it

Thermal pressure

$$p_{\text{th}} = p(n, Y_p, T) - p(n, Y_p, T = 0)$$



“high” densities

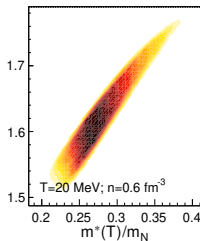
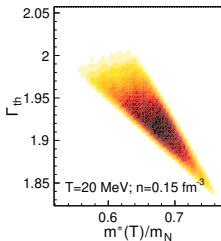
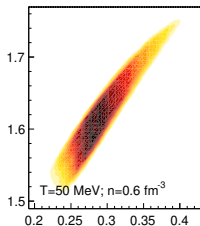
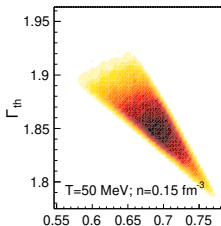
- p_{th} is positively correlated with the Dirac effective mass
- correlations weakening is due to the rearrangement term
- similar quality at low and at high temperatures

“low” densities

- $p_{\text{int}}; p_{\text{th}} > p_{\text{kin}}; p_{\text{th}}$ is negatively correlated with the Dirac effective mass
- the correlation is stronger at high T

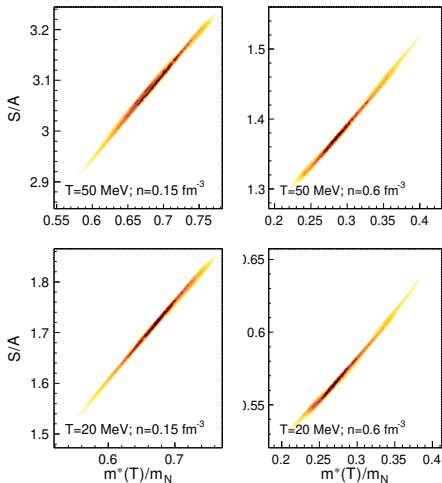
Thermal index

$$\Gamma_{\text{th}} = 1 + p_{\text{th}}/e_{\text{th}}$$



- strong correlations between Γ_{th} and the Dirac effective mass
- two regimes: positive (negative) correlations at "high" ("low") densities similar to the case of p_{th}

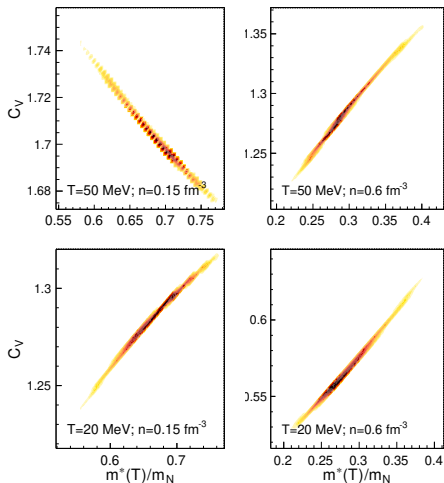
Entropy per nucleon



- excellent, almost linear scaling with Dirac mass
- similar quality at all (n, T)

Heat capacity at constant volume

$$C_V = T (\partial(S/A) / \partial T)_{V, \{N_i\}}$$

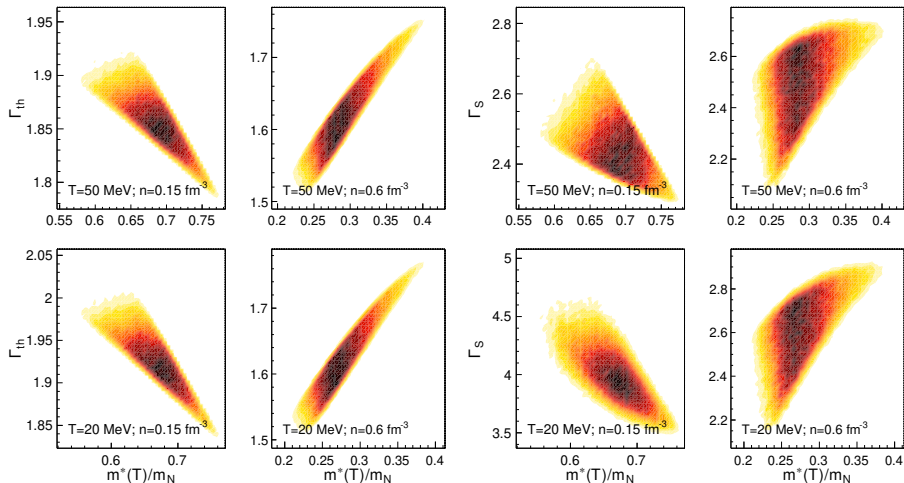


- excellent, almost linear scaling with Dirac mass
- change in sign at low densities and high temperatures

Adiabatic index & speed of sound

$$\Gamma_S = (\partial \ln P / \partial \ln n)_S$$

$$c_S^2 = (dP/de)_{S,A,Y_p} = \Gamma_S P / (e + P)$$



Low temperature approx. (I)

Pseudo-Sommerfeld expansion:

$$e_{\text{kin}}(T) \approx \frac{\mu^*}{8\pi^2} (2\mu^{*2} - m^{*2}) \sqrt{\mu^{*2} - m^{*2}} - \frac{m^{*4}}{8\pi^2} \ln \left(\frac{\sqrt{\mu^{*2} - m^{*2}}}{m^*} + \frac{\mu^*}{m^*} \right) + \frac{1}{6} T^2 \frac{\mu^* (3\mu^{*2} - 2m^{*2})}{(\mu^{*2} - m^{*2})^{1/2}}$$

$$p_{\text{kin}}(T) \approx \frac{\mu^*}{24\pi^2} (2\mu^{*2} - 5m^{*2}) \sqrt{\mu^{*2} - m^{*2}} + \frac{1}{8\pi^2} m^{*4} \ln \left(\frac{\sqrt{\mu^{*2} - m^{*2}}}{m^*} + \frac{\mu^*}{m^*} \right) + \frac{1}{6} T^2 \mu^* (\mu^{*2} - m^{*2})^{1/2}$$

⇒ In this limit, e_{th} , p_{th} , etc. depend effectively only on $m^*(T)$

Numerical results: linear correlations of S/A and e_{th} with $m^*(T)$ survive also beyond this limit; evolution of astro. simulations are expected to depend on $m^*(T)$

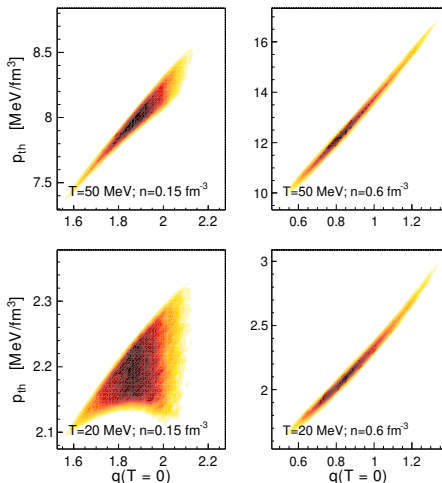
Low temperature approx. (II)

Assuming that $\delta m^*(T) \approx 0$, Constantinou et al. [1] showed that p_{th} , μ_{th} depend on $q = m^{*2}/E_F^{*2} (1 - 3d\ln m^*/d\ln n)$:

$$p_{\text{th}} = \frac{1}{3} anT^2 (1 + q) + \mathcal{O}(T^4); \quad (1)$$

[1] Constantinou, Muccioli, Prakash & Lattimer, Ann. Phys. (2015)

Thermal pressure p_{th}



verified in certain cases

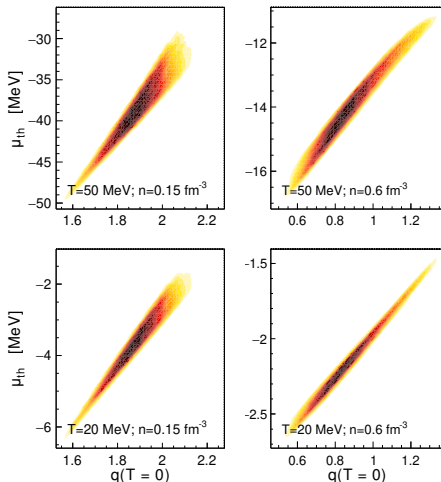
Low temperature approx. (II)

Assuming that $\delta m^*(T) \approx 0$, Constantinou et al. [1] showed that p_{th} , μ_{th} depend on $q = m^{*2}/E_F^{*2} (1 - 3d \ln m^*/d \ln n)$:

$$\mu_{\text{th}} = -\frac{2}{3} a T^2 \left(1 - \frac{q}{2}\right) + \mathcal{O}(T^4)$$

[1] Constantinou, Muccioli, Prakash & Lattimer, Ann. Phys. (2015)

Thermal chemical potential μ_{th}



verified in all these cases, incl. high T

Low temperature approx. (II)

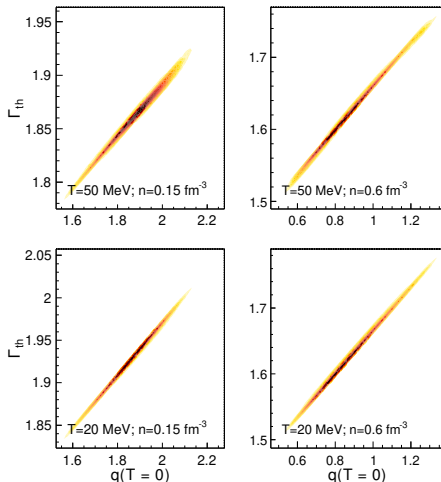
Assuming that $\delta m^*(T) \approx 0$, Constantinou et al. [1] showed that p_{th} , μ_{th} depend on $q = m^{*2}/E_F^{*2} (1 - 3d \ln m^*/d \ln n)$:

$$p_{\text{th}} = \frac{1}{3} a n T^2 (1 + q) + \mathcal{O}(T^4);$$

$$\Gamma_{\text{th}} = 1 + \frac{p_{\text{th}}}{e_{\text{th}}}$$

[1] Constantinou, Muccioli, Prakash & Lattimer, Ann. Phys. (2015)

Thermal index Γ_{th}



excellent scaling, including at high T

Conclusions

- 10^5 Covariant Density Functional EOS models built within a Bayesian approach are used to study finite- T effects in dense matter
- thermal quantities depend on the Dirac effective mass, with e_{th} , S/A being the most sensitive
 - pseudo-Sommerfeld expansion explains the effect, which persists also at high T
- p_{th} , μ_{th} , Γ_{th} are strongly correlated with $q = m^{*2}/E_F^{*2} (1 - 3d \ln m^*/d \ln n)$ [Constantinou+, Ann.Phys. (2015)]
 - the effect persists also at high T and when $\delta m^*(T) \neq 0$
- numerical simulations of CCSN, BNS are expected to show m^* -dependent evolutions
 - similarly to the case of Landau effective mass in non-relativistic models [Yasin+, PRL (2020); Schneider+, ApJ (2020)]